

Extending Cox Proportional Hazards Model with Symbolic Non-Linear Log-Risk Functions for Survival Analysis

Jiaxiang Cheng

School of Electrical and Electronic Engineering
Nanyang Technological University
Singapore
jiaxiang002@e.ntu.edu.sg

Guoqiang Hu

School of Electrical and Electronic Engineering
Nanyang Technological University
Singapore
gqhu@ntu.edu.sg

Abstract—The Cox proportional hazards (CPH) model has been widely applied in survival analysis to estimate relative risks across different subjects given multiple covariates. Traditional CPH models rely on a linear combination of covariates weighted with coefficients as the log-risk function, which imposes a strong and restrictive assumption, limiting generalization. Recent deep learning methods enable non-linear log-risk functions. However, they often lack interpretability due to the end-to-end training mechanisms. The implementation of Kolmogorov-Arnold Networks (KAN) offers new possibilities for extending the CPH model with fully transparent and symbolic non-linear log-risk functions. In this paper, we introduce Generalized Cox Proportional Hazards (GCPH) model, a novel method for survival analysis that leverages KAN to enable a non-linear mapping from covariates to survival outcomes in a fully symbolic manner. GCPH maintains the interpretability of traditional CPH models while allowing for estimation of non-linear log-risk functions. Experiments conducted on both synthetic data and public benchmarks demonstrate that GCPH achieves competitive performance in terms of prediction accuracy and exhibits superior interpretability compared to current state-of-the-art methods.

Index Terms—Survival analysis, Kolmogorov-Arnold Networks, Cox proportional hazards model.

I. INTRODUCTION

Survival analysis is widely applied across various industries to predict survival probabilities and estimate risks over the lifetime of different subjects. One of the most popular models for this purpose is the Cox proportional hazards (CPH) model, which models the relationship between covariates of subjects and their survival outcomes [1]. The *hazard function* in the CPH model is specified as:

$$h(t | \mathbf{x}) = h_0(t)e^{\beta\mathbf{x}}, \quad (1)$$

where t is the time, \mathbf{x} is the covariate vector with coefficients β , and $h_0(t)$ is the baseline hazard function, identical for all subjects. The *hazard ratio*, or relative risk, between two subjects with covariates \mathbf{x}_1 and \mathbf{x}_2 is compared as:

$$\frac{h_1(t | \mathbf{x}_1)}{h_2(t | \mathbf{x}_2)} = \frac{h_0(t)e^{\beta\mathbf{x}_1}}{h_0(t)e^{\beta\mathbf{x}_2}} = \frac{e^{\beta\mathbf{x}_1}}{e^{\beta\mathbf{x}_2}} = e^{\beta(\mathbf{x}_1 - \mathbf{x}_2)}, \quad (2)$$

which is independent of time t and only related to the covariates. Therefore, the CPH model is commonly referred

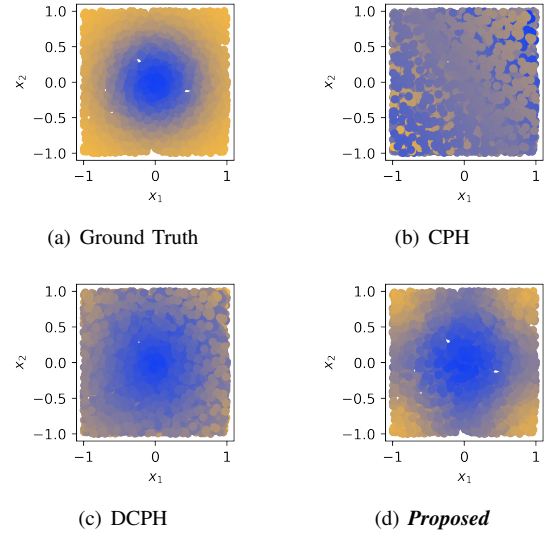


Fig. 1. **Comparison of learning abilities from non-linear relationships.** The experiments are based on synthetic non-linear data, illustrated in (a). The models compared are (b) traditional CPH [1], (c) DCPH [2], and (d) our proposed model. *This demonstrates the enhanced capability of proposed model in capturing non-linear relationships compared to existing methods.*

to as a *semi-parametric model*, as it only requires partial parameters to be specified. The CPH model has been extensively applied due to its efficiency in evaluating relative risks between subjects with different covariates. The term $f(\mathbf{x}; \beta) = \beta\mathbf{x}$ in Equation 1 is also called the *log-risk function*. While this linear assumption in the traditional CPH model simplifies the modeling process regarding parameter estimation, it also highly restricts the generalization ability when dealing with more complex and non-linear relationships. Consequently, recent research has focused on extending the CPH model to incorporate a *non-linear log-risk function*.

Previous work [2], [3] has proposed using neural networks to approximate the log-risk function as $f(\mathbf{x}; \theta)$, where θ are the parameters optimized in the neural networks. Deep neural networks or multi-layer perceptrons (MLP) are effec-

tive in modeling the non-linear relationship between inputs and outputs. However, with increasing concerns about model interpretability, a more transparent survival model is needed to extend the traditional CPH model with generalized non-linearity. Therefore, to overcome the challenges, the main contributions of this paper can be summarized as follows:

- To the best of our knowledge, this is at least one of the first efforts to achieve fully symbolic derivation of the non-linear log-risk function in survival analysis by leveraging the Kolmogorov-Arnold Networks (KAN). This work was completed in Aug 19, 2024, with all experiments and results finalized in a public GitHub repository by the end of the same month¹. Subsequently, a related preprint was published on Sep 6, 2024 [4], which shares a similar model name and approach. And our study provides a complementary perspective.
- We propose a novel method for training a single-layer KAN model through a specialized loss function to approximate the log-risk function and predict hazards for different subjects in the context of survival analysis.
- Extensive experiments are conducted on various synthetic and public benchmarks, which are complementary to experiments by [4], to demonstrate the outstanding performance of our proposed model. The estimated symbolic functions provide new insights into understanding the effects of different variables on survival outcomes.

II. RELATED WORK

1) *Machine Learning for Survival Analysis*: Machine learning (ML) has gained significant attention in recent years for survival analysis [5]. One of the first successful ML-based models for survival analysis is the random survival forests (RSF) method. It handles censored data by introducing new survival splitting rules to the conventional random forests method [6], where the *censored data* are the subjects with events not observed during study. The relevance vector machine was extended to improve computational efficiency and sparsity, thereby learning the nonlinear impacts of covariates on survival outcomes [7]. The deep multi-task Gaussian process (DMGP) was also utilized to model the relationships between input covariates and survival times [8]. In recent years, deep learning-based models have been widely proposed to handle large-scale data due to their outstanding ability to learn complex relationships among covariates. DeepHit models the *time to event* as the hitting time in a stochastic process, rather than modeling it in continuous-time space [9], whereas Nnet-survival models survival times in discrete-time space [10]. Additionally, graph convolutional networks have also been applied to survival analysis to capture local neighbors from high-dimensional inputs [11].

2) *Extended Cox with Modified Log-Risk Function*: The CPH model continues to receive significant attention and has been extended for multi-tasking [12] and incorporating multi-modal data [13]. Following the original practice of

using neural networks for modeling survival data in [3], both DCPH (DeepSurv) and Cox-nnet combine modern deep neural networks with the inference mechanism of the CPH model to extract the impacts of different features on the hazard ratio [2], [14]. However, deep learning models often lack transparency and interpretability, which are major concerns in critical scenarios. The end-to-end training mechanisms pose challenges in uncovering the underlying principles of the relationships between predictors and response variables.

III. METHODOLOGY

In this section, we introduce the proposed model, which adapts KAN for approximating the log-risk function in survival analysis. We also present the specialized loss function that enables the prediction of survival outcomes.

A. Model Architecture

In this paper, instead of using deep learning models to approximate the log-risk function, we employ the KAN for symbolic approximation. Unlike deep neural networks, KAN directly estimates the linear or non-linear *activation function* from each v -th feature x_v to the log-risk as:

$$f(\mathbf{x}; \Phi) = \sum_{v=1}^V \phi_v(x_v), \quad (3)$$

which is equivalent to employing a single layer of KAN with a size of V (*i.e.*, the number of covariates) as formulated in [15], with model architecture illustrated in Figure 2. For each covariate x_v , we approximate an independent function $\phi_v(\cdot)$, and the log-risk function is the summation of the outputs from all activations.

1) *Optimization*: To enable an optimizable activation function, each $\phi_v(\cdot)$ is defined as [15]:

$$\phi_v(x_v) = \omega_v^b b(x_v) + \omega_v^s S_v(x_v), \quad (4)$$

where $b(x)$ is a *basis function* and $S_v(x)$ is the *spline function*, defined and formulated as:

$$b(x_v) = \frac{x_v}{1 + e^{-x_v}}, \quad (5)$$

$$S_v(x_v) = \sum_{k=1}^K c_{v,k} B_{v,k}(x_v), \quad (6)$$

respectively. Here, $S_v(x)$ is a linear combination of *B-splines*, *i.e.*, $B_{v,k}(x_v)$, with K the order. The scales of $b(x)$ and $S_v(x)$, *i.e.*, ω_v^b and ω_v^s , and scales of $B_{v,k}(x_v)$, *i.e.*, $c_{v,k}$, are the trainable parameters.

2) *Symbolification*: To enable an explainable and transparent non-linear log-risk function, we employ the *symbolification* process introduced in [15]. The process is straightforward: after the optimization process, we use several candidate symbolic functions $y(x)$ to approximate the optimized $\hat{\phi}_v(x)$ in the form:

$$\hat{\phi}_v(x_v) \approx \alpha_3 y(\alpha_1 x_v + \alpha_2) + \alpha_4, \quad (7)$$

where $(\alpha_1, \alpha_2, \alpha_3, \alpha_4)$ are *affine parameters* to be fitted. The optimal symbolic function $y_v^*(x)$ is then selected based on the best fitting performance, evaluated using R^2 .

¹<https://github.com/jxiang-cheng/KAN-for-Survival-Analysis>

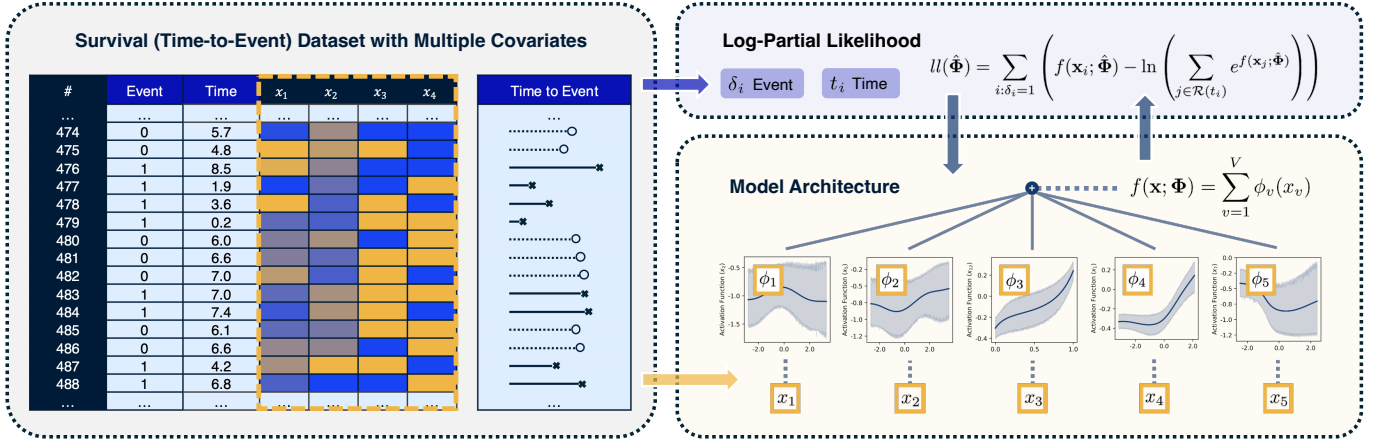


Fig. 2. Overview of proposed GCPH for survival analysis by extending CPH model with non-linear symbolic log-risk function. A typical survival dataset is presented and used for training the GCPH with a specialized loss function, including the *log-partial likelihood function*. Confidence interval is also illustrated for each *symbolic activation function* through multiple tests with different random seeds for initialization.

B. Loss Function

A specialized loss function is proposed that enables the KAN to approximate the non-linear log-risk function, which consists of log-partial likelihood function aligned with CPH model and regularization loss for preventing overfitting.

1) *Log-Partial Likelihood*: In the CPH model, the *partial likelihood function* is constructed to optimize the coefficients β in Equation 1, formulated as follows:

$$l(\hat{\beta}) = \prod_{i:\delta_i=1} \frac{e^{f(\mathbf{x}_i;\hat{\beta})}}{\sum_{j \in \mathcal{R}(t_i)} e^{f(\mathbf{x}_j;\hat{\beta})}}, \quad (8)$$

where the product is taken over each i -th subjects where the event has occurred ($\delta_i = 1$) and $\mathcal{R}(t_i)$ denotes the set of subjects still at risk at time t_i , *i.e.*, without events occurred by the time t_i . This function represents the probability of the event occurring for the i -th subject, given the total number of subjects still at risk at time t_i (*i.e.*, the *survival time* of the i -th subject). The regression is performed by maximizing the partial likelihood function $l(\hat{\beta})$.

Similarly, for training the KAN model, we define the *log-partial likelihood function* given the estimated $\hat{\Phi}$ as:

$$ll(\hat{\Phi}) = \sum_{i:\delta_i=1} \left(f(\mathbf{x}_i; \hat{\Phi}) - \ln \left(\sum_{j \in \mathcal{R}(t_i)} e^{f(\mathbf{x}_j; \hat{\Phi})} \right) \right) \quad (9)$$

2) *Regularization Loss*: Regularization is applied as developed in [15] to encourage sparsity and prevent overfitting of the KAN. Given an input batch \mathcal{B} , for each activation function ϕ_v , the $L1$ norm is calculated as:

$$\|\hat{\phi}_v\|_1 = \frac{1}{|\mathcal{B}|} \sum_{\mathbf{x} \in \mathcal{B}} |\hat{\phi}_v(x_v)|, \quad \text{and} \quad (10)$$

$$\|\hat{\Phi}\|_1 = \sum_{v=1}^V \|\hat{\phi}_v\|_1, \quad (11)$$

where the $L1$ norm of the estimated $\hat{\Phi}$ is calculated as the summation of the $L1$ norms of all activation functions.

Additionally, an *entropy loss* is also introduced in [15] and formulated as follows:

$$H(\hat{\Phi}) = - \sum_{v=1}^V \frac{\|\hat{\phi}_v\|_1}{\|\hat{\Phi}\|_1} \ln \left(\frac{\|\hat{\phi}_v\|_1}{\|\hat{\Phi}\|_1} \right). \quad (12)$$

The *regularization loss* is the summation of the $L1$ norm of $\hat{\Phi}$ and the entropy regularization loss:

$$\mathcal{L}_{\text{reg}}(\hat{\Phi}) = \mu_1 \|\hat{\Phi}\|_1 + \mu_2 H(\hat{\Phi}), \quad (13)$$

where μ_1 and μ_2 are the weights assigned to the $L1$ norm and entropy regularization loss, respectively.

Thus, the total loss function is a combination of the *negative log-partial likelihood* and the regularization loss:

$$\mathcal{L} = -ll(\hat{\Phi}) + \gamma \mathcal{L}_{\text{reg}}(\hat{\Phi}), \quad (14)$$

where γ is the weight assigned to the regularization loss.

IV. EXPERIMENTS

We conducted extensive experiments with our proposed model on both synthetic data and public benchmark and compared to different baseline models.

A. Datasets

We first generate synthetic data following practices in [2] with known linear and non-linear log-risk.

1) *Synthetic Linear Data*: We generate synthetic data where subjects have a linear log-risk function given by:

$$f(\mathbf{x}) = x_1 + 2x_2. \quad (15)$$

2) *Synthetic Non-Linear Data*: We also generate synthetic data with a known non-linear log-risk function:

$$f(\mathbf{x}) = \ln(\lambda) \exp \left(-\frac{x_1^2 + x_2^2}{2r^2} \right), \quad (16)$$

where we set the parameters $\lambda = 5$ and $r = 2$, also aligned with the settings in [2].

TABLE I
SUMMARY OF EXPERIMENTAL RESULTS COMPARING PROPOSED METHOD WITH DIFFERENT BASELINE MODELS. C-INDEX AND BRIER SCORE COMPUTED WITH THE PREDICTIONS BY DIFFERENT MODELS ON VARIOUS BENCHMARK.

Data	Model	C-Index \uparrow			Brier Score \downarrow		
		25%	50%	75%	25%	50%	75%
Synthetic Linear	CPH	0.795 (0.013)	0.787 (0.013)	0.779 (0.011)	0.128 (0.007)	0.150 (0.011)	0.124 (0.010)
	RSF	0.762 (0.014)	0.770 (0.013)	0.761 (0.011)	0.141 (0.007)	0.162 (0.011)	0.133 (0.013)
	DCPH	0.794 (0.013)	0.786 (0.012)	0.778 (0.010)	0.128 (0.006)	0.151 (0.011)	0.125 (0.011)
	DCM	0.793 (0.013)	0.786 (0.012)	0.778 (0.011)	0.128 (0.006)	0.151 (0.011)	0.125 (0.010)
	DSM	0.792 (0.012)	0.785 (0.014)	0.776 (0.012)	0.128 (0.006)	0.151 (0.011)	0.128 (0.012)
	GCPH	0.793 (0.015)	0.783 (0.012)	0.774 (0.010)	0.129 (0.008)	0.153 (0.013)	0.129 (0.011)
	GCPH-l	0.796 (0.013)	0.788 (0.013)	0.779 (0.011)	0.128 (0.007)	0.150 (0.012)	0.124 (0.011)
Synthetic Non-Linear	CPH	0.496 (0.030)	0.500 (0.022)	0.501 (0.020)	0.176 (0.011)	0.248 (0.003)	0.220 (0.006)
	RSF	0.587 (0.023)	0.582 (0.023)	0.584 (0.017)	0.178 (0.012)	0.250 (0.010)	0.221 (0.009)
	DCPH	0.626 (0.030)	0.619 (0.018)	0.616 (0.016)	0.168 (0.011)	0.229 (0.004)	0.200 (0.007)
	DCM	0.620 (0.027)	0.614 (0.016)	0.612 (0.016)	0.171 (0.011)	0.236 (0.005)	0.207 (0.009)
	DSM	0.560 (0.045)	0.554 (0.060)	0.550 (0.062)	0.175 (0.012)	0.247 (0.007)	0.218 (0.006)
	GCPH	0.624 (0.028)	0.616 (0.018)	0.611 (0.016)	0.167 (0.013)	0.230 (0.005)	0.202 (0.009)
TRACE	CPH	0.757 (0.031)	0.742 (0.020)	0.738 (0.013)	0.093 (0.008)	0.155 (0.010)	0.180 (0.007)
	RSF	0.737 (0.030)	0.738 (0.017)	0.728 (0.008)	0.096 (0.008)	0.158 (0.010)	0.186 (0.006)
	DCPH	0.762 (0.029)	0.749 (0.020)	0.742 (0.013)	0.092 (0.008)	0.152 (0.011)	0.178 (0.007)
	DCM	0.753 (0.034)	0.744 (0.019)	0.737 (0.011)	0.094 (0.008)	0.153 (0.010)	0.180 (0.004)
	DSM	0.753 (0.030)	0.738 (0.018)	0.731 (0.012)	0.094 (0.009)	0.159 (0.008)	0.185 (0.006)
	GCPH	0.761 (0.029)	0.747 (0.019)	0.741 (0.013)	0.093 (0.008)	0.154 (0.010)	0.179 (0.007)
COLON	CPH	0.700 (0.022)	0.670 (0.036)	0.663 (0.036)	0.106 (0.014)	0.171 (0.016)	0.206 (0.016)
	RSF	0.668 (0.025)	0.651 (0.026)	0.657 (0.030)	0.109 (0.013)	0.176 (0.015)	0.208 (0.016)
	DCPH	0.676 (0.031)	0.650 (0.033)	0.649 (0.033)	0.108 (0.013)	0.175 (0.015)	0.211 (0.013)
	DCM	0.683 (0.027)	0.649 (0.040)	0.653 (0.039)	0.111 (0.014)	0.178 (0.015)	0.218 (0.012)
	DSM	0.704 (0.024)	0.667 (0.032)	0.660 (0.036)	0.107 (0.014)	0.175 (0.018)	0.212 (0.017)
	GCPH	0.703 (0.028)	0.668 (0.039)	0.666 (0.036)	0.106 (0.013)	0.171 (0.016)	0.205 (0.016)
RDATA	CPH	0.668 (0.035)	0.673 (0.026)	0.674 (0.020)	0.103 (0.015)	0.177 (0.014)	0.205 (0.012)
	RSF	0.644 (0.020)	0.647 (0.025)	0.653 (0.025)	0.109 (0.014)	0.187 (0.018)	0.218 (0.016)
	DCPH	0.666 (0.032)	0.672 (0.028)	0.674 (0.021)	0.103 (0.015)	0.176 (0.014)	0.206 (0.011)
	DCM	0.661 (0.035)	0.668 (0.029)	0.670 (0.023)	0.103 (0.016)	0.179 (0.014)	0.209 (0.010)
	DSM	0.663 (0.037)	0.667 (0.027)	0.669 (0.023)	0.102 (0.016)	0.177 (0.015)	0.207 (0.013)
	GCPH	0.666 (0.029)	0.674 (0.027)	0.676 (0.023)	0.103 (0.014)	0.176 (0.014)	0.206 (0.013)
FRTCS	CPH	0.727 (0.131)	0.695 (0.119)	0.704 (0.107)	0.025 (0.011)	0.052 (0.017)	0.074 (0.022)
	RSF	0.461 (0.130)	0.625 (0.095)	0.651 (0.088)	0.026 (0.011)	0.052 (0.016)	0.072 (0.019)
	DCPH	0.644 (0.169)	0.672 (0.139)	0.700 (0.109)	0.025 (0.011)	0.052 (0.017)	0.072 (0.022)
	DCM	0.656 (0.159)	0.671 (0.103)	0.628 (0.079)	0.025 (0.011)	0.051 (0.016)	0.072 (0.019)
	DSM	0.677 (0.151)	0.672 (0.144)	0.664 (0.132)	0.025 (0.011)	0.051 (0.016)	0.072 (0.020)
	GCPH	0.711 (0.178)	0.718 (0.106)	0.727 (0.081)	0.020 (0.005)	0.047 (0.016)	0.069 (0.021)

In both synthetic datasets, each x_v is simulated from a *uniform distribution*, *i.e.*, $U(-1, 1)$. The initial death time t_0 is simulated from an *exponential distribution* with a mean of 5, while the death time t is derived as $t = t_0 / \exp(f(\mathbf{x}))$. The simulated time is then capped so that 10% of subjects are censored with no events observed [2].

3) *TRACE*: The TRACE dataset studies survival probability of patients after myocardial infarction [16] and includes 1,878 patients [17] with a censoring rate of 48.99% (*i.e.*, percentage of patients without events occurred). It features four binary variables: *sex* (1 if female), clinical heart pump failure (*chf*, 1 if present), *diabetes* (1 if present), and ventricular fibrillation (*vf*, 1 if present). Additionally, it contains two numerical variables: *wmi* (a measure of heart pumping effect based on ultrasound, where 2 is normal and 0 is worst) and *age*.

4) *COLON*: The COLON dataset examines adjuvant chemotherapy for colon cancer [18], [19] and comprises 929 patients with a censoring rate of 51.35%. It includes five binary variables: *sex* (M if male, F if female), obstruction of colon by tumor (*obstruct*, Y or N), perforation of colon (*perfor*, Y or N), adherence to nearby organs (*adhere*, Y or N), and more than 4 positive lymph nodes (*node4*, Y or N). There are also two categorical variables: treatment (*rx*, with *Obs* for observation, *Lev* for Levamisole, and *Lev+5-FU* for Levamisole+5-FU) and tumor differentiation (*differ*, with levels *well*, *moderate*, and *poor*). Additionally, it contains two numerical variables: *age* and number of lymph nodes with detectable cancer (*nodes*).

5) *RDATA*: The RDATA dataset includes 1,040 subjects with a censoring rate of 47.40% [20]. It features one categorical variable: *agegr* (age group), one binary variable: *sex*

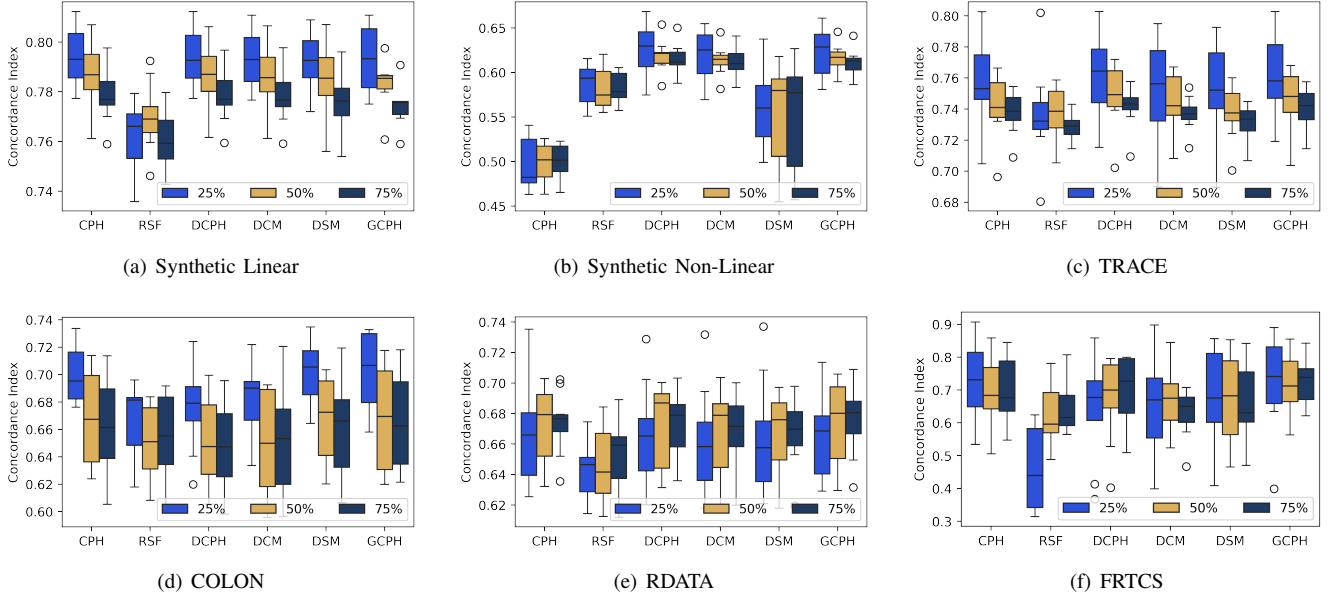


Fig. 3. **Box plots of C-Index evaluated on the prediction results by different models**, on various datasets including (a) synthetic linear data, (b) synthetic non-linear data, (c) TRACE, (d) COLON, (e) RDATA, and (f) FRTCS.

(1 if male, 2 if female), and two numerical variables: *age* and *date of diagnosis (year)*.

6) *FRTCS*: The French Three Cities Study (FRTCS) dataset contains 697 subjects with a censoring rate of 89.67% [21]. It includes four binary variables: *sex* (M if male, F if female) and use of antihypertensive drugs (*antihyp0* to *antihyp2*, Y or N). Additionally, it features nine numerical variables: *age*, three records of systolic blood pressure (*sbp0* to *sbp2*), three records of diastolic blood pressure (*dbp0* to *dbp2*), and two records of dates (*date0* and *date1*).

B. Model Settings

In our model, the number of activation functions is set to match the number of covariates in each dataset, *i.e.*, V . The weights for the $L1$ norm and entropy regularization losses are set to $\mu_1 = 1$ and $\mu_2 = 10$ in Equation 13. Additionally, the weight for the total regularization loss is set to $\gamma = 0.1$ in Equation 14. And for spline functions, we set an order of 3, *i.e.*, $k = 3$ in Equation 6, and a total of 5 intervals for each spline function. We select the symbolic functions as $y(x)$ for approximation, including x , x^2 , x^3 , x^4 , \exp , \ln , $\sqrt{\cdot}$, \tanh , \sin . We also test *Linear GCPH* by using only x to fit activation functions, denoted as *GCPH-l*.

The baseline models we experimented and compared with include CPH [1], RSF [6], DCPH [2], DCM [22], and DSM [23].

C. Evaluation Metrics

1) *Concordance Index (C-Index)*: The C-Index assesses how well the predicted risk scores align with the actual survival times. Given a dataset with n pairs of instances (i, j) , where each instance i has a survival time t_i and an event

indicator δ_i , and \hat{r}_i denotes the predicted risk score for instance i , the C-Index is defined as:

$$CI = \frac{\sum_{i < j} I(t_i < t_j) \cdot I(\hat{r}_i > \hat{r}_j) \cdot (\delta_i + \delta_j)}{\sum_{i < j} I(t_i < t_j) \cdot (\delta_i + \delta_j)}, \quad (17)$$

where $I(\cdot)$ is an indicator function that returns 1 if the condition is met and 0 otherwise. The numerator counts the number of concordant pairs, and the denominator normalizes by the total number of comparable pairs.

2) *Brier Score*: It measures the accuracy of probabilistic predictions, taking into account both the calibration and discrimination of the model. It is defined as the *mean squared error* between the predicted survival probability and the actual outcome. For a survival model, the Brier Score at a specific time point t can be written as:

$$\text{Brier Score}(t) = \frac{1}{n} \sum_{i=1}^n \frac{(\hat{S}(t | \mathbf{x}_i) - I(t_i > t))^2}{\hat{G}(t | \mathbf{x}_i)}, \quad (18)$$

where $\hat{S}(t | \mathbf{x}_i)$ is the predicted survival probability for instance i at time t . And $\hat{G}(t | \mathbf{x}_i)$ is the Kaplan-Meier estimate of the survival function of the censoring distribution.

In our experiments, we choose the 25, 50, and 75-th percentiles of time t_i in the train data as the time t to compare the Brier Score, as well as the C-Index. A higher C-Index indicates better performance of the model and a C-Index of 0.5 corresponds to random chance. A lower Brier Score indicates better accuracy of the probabilistic predictions.

D. Experimental Results

The experimental results using different models on various datasets are summarized in Table I with corresponding C-index

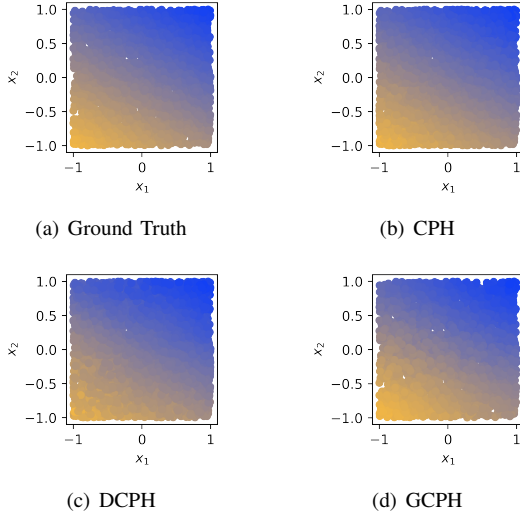


Fig. 4. **Comparison of learning abilities from linear relationships.** The experiments are based on synthetic non-linear data, illustrated in (a). The models compared are (b) traditional CPH [1], (c) DCPH [2], and (d) our proposed GCPH model.

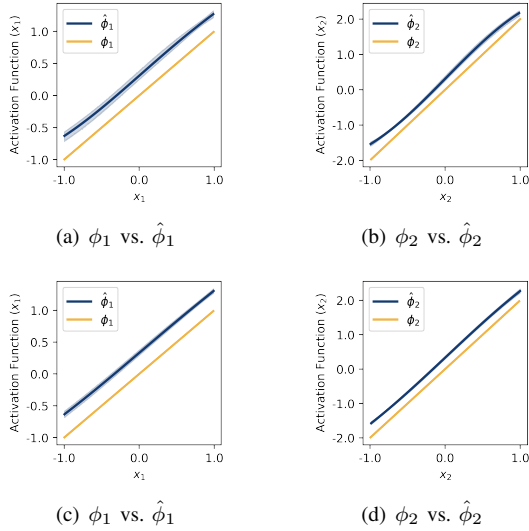


Fig. 5. **Symbolic functions learned by GCPH (a-b) and GCPH-l (c-d) compared to ground truth in the linear experiments.** $\phi_1(x) = x$ and $\phi_2(x) = 2x$, while $\hat{\phi}_1$ and $\hat{\phi}_2$ are the predicted ones with multiple runs.

and Brier Score evaluated. We also illustrate the results on C-index in Figure 3 with box plots. It can be seen that our proposed model achieves competitive performance.

1) *Linear and Non-Linear Experiments:* In linear experiments, the CPH model performs well due to its inherent linear assumption, while GCPH-l achieves the optimal performance as shown in Table I. For non-linear experiments, DCPH achieves the best performance, with the proposed GCPH coming in a close second. Despite having much fewer trained parameters (2 hidden layers with 100 neurons adopted for DCPH), GCPH delivers competitive results with its much simpler and more transparent architecture.

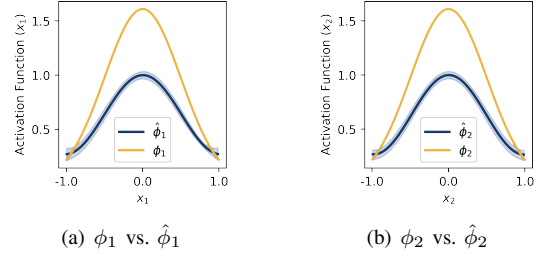


Fig. 6. **Symbolic functions learned by GCPH compared to ground truth in the non-linear experiments.** $\phi_1(x) = \phi_2(x) = \ln(\lambda) \exp(-0.5x^2/r^2)$, while $\hat{\phi}_1$ and $\hat{\phi}_2$ are the predicted ones with multiple runs.

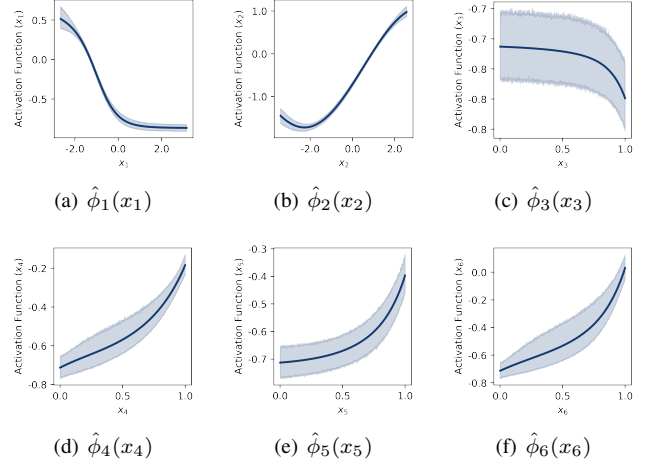


Fig. 7. **Symbolic functions learned by GCPH with TRACE dataset.** Variables from (a) x_1 to (f) x_6 represent *wmi*, *age*, *sex*, presence of *chf*, *diabetes*, and *vf*, respectively.

Figures 4 and 1 illustrate the prediction results for linear and non-linear experiments, respectively. In Figure 4(a), the true linear relationship is shown, and CPH, DCPH, and GCPH effectively capture this relationship. GCPH's predictions are notably less noisy, as compared between Figures 4(c) and 4(d). In non-linear experiments, depicted in Figure 1, the differences in model performance are more pronounced. The CPH model struggles with the non-linear relationships due to its linear assumptions, while GCPH closely matches the ground truth shown in Figure 1(a).

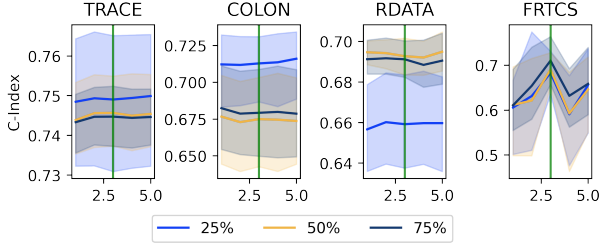
Figures 5 and 6 present the symbolic functions estimated by GCPH for each variable. Each symbolic function $\hat{\phi}_v(x_v)$ is obtained by setting all other variables in $f(\mathbf{x}; \hat{\Phi})$ to 0, *i.e.*, $\hat{\phi}_v(x_v) = f(x_v, x_{s:s \neq v} = 0; \hat{\Phi})$. These symbolic functions closely approximate the ground truth, effectively reflecting the actual shape of the relationships.

2) *Experiments with Real-World Data:* The results from experiments on real-world datasets, namely TRACE, COLON, RDATA, and FRTCS, are also summarized in Table I and Figure 3. These results demonstrate the competitive performance of GCPH. While DCPH achieves the best performance on TRACE, with GCPH as the second-best, GCPH performs within half of the best results in the remaining datasets.

TABLE II

SUMMARY OF SYMBOLIC NON-LINEAR LOG-RISK FUNCTION APPROXIMATED WITH DIFFERENT PUBLIC BENCHMARK. TWO FLOATING DIGITS ARE RESERVED TO SIMPLIFY THE SYMBOLIC FUNCTIONS WHILE SHOWING THE MOST IMPORTANT FEATURES.

Data	Symbolic Non-Linear Log-Risk Function
TRACE	$f(\mathbf{x}; \hat{\Phi}) = -1.6\text{tanh}(0.5x_1 + 1.1) - 1.3\sin(0.5x_2 + 9.3) + 0.9$, $x_1: wmi, x_2: age$
COLON	$f(\mathbf{x}; \hat{\Phi}) = 0.2\text{tanh}(1.4x_1 - 0.6) + 0.5\text{tanh}(0.7x_2) - 0.2$, $x_1: age, x_2: \text{number of lymph nodes}$
RDATA	$f(\mathbf{x}; \hat{\Phi}) = 1.6\text{tanh}(0.4x_1 + 0.2) - 0.2\text{tanh}(3.9x_2 - 1.1) + 0.1(x_5 + 0.5)^4 - 0.3$, $x_1: age, x_2: \text{date of diagnosis}, x_5: \text{if in age group within 71 to 95 years old}$
FRTCS	$f(\mathbf{x}; \hat{\Phi}) = 0.2\sin(1.4x_1 + 6.8) - 0.2\sin(1.6x_2 + 5.2) - 0.6\text{tanh}(1.2x_3 + 1.3) - 0.8\sin(1.2x_4 - 2.6)$ $- 0.2\sin(1.8x_5 - 10) + 0.2(x_6 + 1)^2 - 0.5\text{tanh}(2.3x_7 + 2) + 0.4\text{tanh}(1x_8 + 0.2) + 0.6(x_{12} + 0.2)^4 - 1.2$, $x_1: age, x_2: sbp0, x_3: dbp0, x_4: sbp1, x_5: dbp1, x_6: sbp2, x_7: dbp2, x_8: date0, x_{12}: antihyp1$



(a) Impacts of order setting in spline function

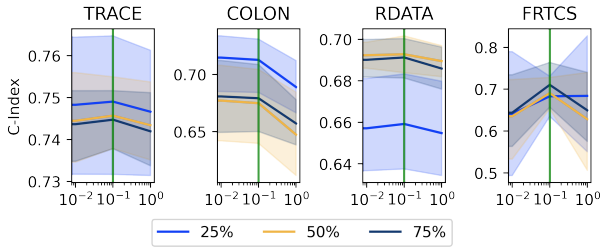
(b) Impacts of γ setting in loss function

Fig. 8. Ablation study on model configurations on real-world datasets, including impacts of (a) order setting in spline function and (b) regularization term in loss function.

Additionally, GCPH provides symbolic functions that illustrate the relationships between covariates and risk of patients.

Figure 7 presents the symbolic functions estimated for each variable in TRACE. The variables include the measure of heart pumping effect (*wmi*, where 2 is normal and 0 is worst), age, sex (1 if female), clinical heart pump failure (*chf*, 1 if present), diabetes (1 if present), and ventricular fibrillation (*vf*, 1 if present). The estimated functions indicate that the presence of clinical heart pump failure, diabetes, or ventricular fibrillation increases patient risk. Conversely, a higher measure of heart pumping effect is associated with lower risk, and older patients face higher risk. Gender appears to have less impact on risk, as shown in Figure 7(c).

We summarize the symbolic non-linear log-risk functions approximated by GCPH for various public benchmarks in Table II. For simplicity, we present the functions with only two decimal places, excluding activation functions with minimal weights to highlight important features.

E. Ablation Study

We conducted an ablation study to evaluate the impact of different model configurations in our experiments.

1) *Impact of Order Setting*: Figure 8(a) shows the model performance using varying spline function orders, ranging from 1 to 5, with $\gamma = 0.1$. The results indicate that the model performance is generally less sensitive to changes in order. However, significant impacts were observed on the FRTCS dataset, with the setting of $K = 3$ yielding optimal performance in our experiments.

2) *Impact of Regularization Loss*: We also evaluated the impact of the regularization term in the loss function by varying γ . As shown in Figure 8(b), the regularization term has a more pronounced effect across different datasets compared to the order setting. Overall, our choice of $\gamma = 0.1$ provided the best performance among the configurations tested.

V. CONCLUSION

In this paper, we propose an extended CPH model that incorporates a symbolic non-linear log-risk function. This function is approximated using the KAN model, allowing for an effective symbolic representation of the relationships between covariates and survival outcomes. We integrate the log-partial likelihood function into the loss function to update the GCPH model, enabling it to perform survival analysis. Compared to extended CPH models using MLPs, which often involve many trainable parameters and lack interpretability, our model offers a transparent and streamlined formulation of the log-risk function. This approach provides valuable insights into how different variables influence survival outcomes in an interpretable manner.

REFERENCES

- [1] D. R. Cox. Regression Models and Life-Tables. *Journal of the Royal Statistical Society. Series B (Methodological)*, 34(2):187–220, 1972. Publisher: [Royal Statistical Society, Wiley].
- [2] Jared L. Katzman, Uri Shaham, Alexander Cloninger, Jonathan Bates, Tingting Jiang, and Yuval Kluger. DeepSurv: personalized treatment recommender system using a Cox proportional hazards deep neural network. *BMC Medical Research Methodology*, 18(1):24, February 2018.
- [3] David Faraggi and Richard Simon. A neural network model for survival data. *Statistics in Medicine*, 14(1):73–82, January 1995.
- [4] William Knottenbelt, Zeyu Gao, Rebecca Wray, Woody Zhidong Zhang, Jiashuai Liu, and Mireia Crispin-Ortuzar. CoxKAN: Kolmogorov-Arnold Networks for Interpretable, High-Performance Survival Analysis, September 2024. arXiv:2409.04290 [cs].

- [5] Ping Wang, Yan Li, and Chandan K. Reddy. Machine Learning for Survival Analysis: A Survey. *ACM Computing Surveys*, 51(6):1–36, November 2019.
- [6] Hemant Ishwaran, Udaya B. Kogalur, Eugene H. Blackstone, and Michael S. Lauer. Random survival forests. *The Annals of Applied Statistics*, 2(3):841–860, September 2008. Publisher: Institute of Mathematical Statistics.
- [7] Farkhondeh Kiaee, Hamid Sheikhzadeh, and Samaneh Eftekhari Mahabadi. Relevance Vector Machine for Survival Analysis. *IEEE Transactions on Neural Networks and Learning Systems*, 27(3):648–660, March 2016. Conference Name: IEEE Transactions on Neural Networks and Learning Systems.
- [8] Ahmed M. Alaa and Mihaela van der Schaar. Deep multi-task Gaussian processes for survival analysis with competing risks. In *Proceedings of the 31st International Conference on Neural Information Processing Systems, NIPS’17*, pages 2326–2334, Red Hook, NY, USA, December 2017. Curran Associates Inc.
- [9] Changhee Lee, William Zame, Jinsung Yoon, and Mihaela van der Schaar. DeepHit: A Deep Learning Approach to Survival Analysis With Competing Risks. *Proceedings of the AAAI Conference on Artificial Intelligence*, 32(1), April 2018. Number: 1.
- [10] Michael F. Gensheimer and Balasubramanian Narasimhan. A scalable discrete-time survival model for neural networks. *PeerJ*, 7:e6257, January 2019. Publisher: PeerJ Inc.
- [11] Yurong Ling, Zijing Liu, and Jing-Hao Xue. Survival Analysis of High-Dimensional Data With Graph Convolutional Networks and Geometric Graphs. *IEEE Transactions on Neural Networks and Learning Systems*, pages 1–11, 2022. Conference Name: IEEE Transactions on Neural Networks and Learning Systems.
- [12] Cheng Liu, Wenming Cao, Si Wu, Wenjun Shen, Dazhi Jiang, Zhiwen Yu, and Hau-San Wong. Asymmetric Graph-Guided Multitask Survival Analysis With Self-Paced Learning. *IEEE Transactions on Neural Networks and Learning Systems*, 33(2):654–666, February 2022. Conference Name: IEEE Transactions on Neural Networks and Learning Systems.
- [13] Zhenyuan Ning, Zehui Lin, Qing Xiao, Denghui Du, Qianjin Feng, Wufan Chen, and Yu Zhang. Multi-Constraint Latent Representation Learning for Prognosis Analysis Using Multi-Modal Data. *IEEE Transactions on Neural Networks and Learning Systems*, 34(7):3737–3750, July 2023. Conference Name: IEEE Transactions on Neural Networks and Learning Systems.
- [14] Travers Ching, Xun Zhu, and Lana X. Garmire. Cox-nnet: An artificial neural network method for prognosis prediction of high-throughput omics data. *PLOS Computational Biology*, 14(4):e1006076, April 2018. Publisher: Public Library of Science.
- [15] Ziming Liu, Yixuan Wang, Sachin Vaidya, Fabian Ruehle, James Halverson, Marin Soljačić, Thomas Y. Hou, and Max Tegmark. KAN: Kolmogorov-Arnold Networks, May 2024. arXiv:2404.19756 [cond-mat, stat].
- [16] G. V. H. Jensen, C. Torp-Pedersen, P. Hildebrandt, L. Kober, F. E. Nielsen, T. Melchior, T. Joen, and P. K. Andersen. Does in-hospital ventricular fibrillation affect prognosis after myocardial infarction? *European Heart Journal*, 18(6):919–924, June 1997.
- [17] Thomas Scheike with contributions from Torben Martinussen and Jeremy Silver and Klaus Holst. timereg: Flexible Regression Models for Survival Data, January 2023.
- [18] Charles G. Moertel, Thomas R. Fleming, John S. Macdonald, Daniel G. Haller, John A. Laurie, Catherine M. Tangen, James S. Ungerleider, William A. Emerson, Douglass C. Tormey, John H. Glick, Michael H. Veeder, and James A. Mailliard. Fluorouracil plus Levamisole as Effective Adjuvant Therapy after Resection of Stage III Colon Carcinoma: A Final Report. *Annals of Internal Medicine*, 122(5):321–326, March 1995. Publisher: American College of Physicians.
- [19] Terry M. Therneau, Lumley, Thomas, Atkinson Elizabeth, and Crowson Cynthia. survival: Survival Analysis, June 2024.
- [20] Maja Pohar Perme and Damjan Manevski. relsurv: Relative Survival, December 2022.
- [21] David Hosmer. *Applied Survival Analysis: Regression Modeling of Time to Event Data, 2nd Edition [electronic resource]*. Wiley-Interscience, 1st edition edition, 2008.
- [22] Chirag Nagpal, Steve Yadlowsky, Negar Rostamzadeh, and Katherine Heller. Deep Cox Mixtures for Survival Regression. In *Proceedings of the 6th Machine Learning for Healthcare Conference*, pages 674–708. PMLR, October 2021. ISSN: 2640-3498.
- [23] Chirag Nagpal, Xinyu Li, and Artur Dubrawski. Deep Survival Machines: Fully Parametric Survival Regression and Representation Learning for Censored Data With Competing Risks. *IEEE Journal of Biomedical and Health Informatics*, 25(8):3163–3175, August 2021.